

ECE 445 Design Document

Vision-driven Automatic Posture Correction Device

Team #21

Weichong Chen, Xiaoyu Xu, Yilun Chen

TA: Ruolin Zhao

April 6, 2026

Contents

1	Introduction	4
1.1	Problem and Solution	4
1.2	Visual Aid	4
1.3	High-Level Requirements	4
2	Design Procedure and Alternatives	6
2.1	Sensing Alternatives: Ultrasonic vs. Computer Vision	6
2.2	Actuation Alternatives: Belt Drive vs. Linear Actuator	6
3	System Design	7
3.1	Block Diagram	7
3.2	Physical Design Figures	8
3.3	Physical and Mechanical Design	9
3.4	Electrical Design and Power Budget	9
3.5	Software and Control Design	9
3.6	FSM State Descriptions	10
4	Subsystem Requirements and Verifications	11
4.1	Power Subsystem	11
4.2	Perception Subsystem (Camera, Mic, IMU)	12
4.3	Actuation Subsystem	13
4.4	Software Subsystem	13
4.5	Subsystem Interfaces and Interactions	14
4.5.1	Key Signal and Power Flows	15
4.6	Supporting Materials–Design Calculations and Justifications	16
4.6.1	Discrete PID Control Strategy	16
4.6.2	I2C Communication Bandwidth	16
5	Tolerance Analysis	16
5.1	Actuator Thrust and Pitch Motor Torque Analysis	16
5.2	Mechanical Resolution and Stability Tolerance	17

6	Cost and Schedule	18
6.1	Cost Analysis	18
6.1.1	Labor	18
6.1.2	Parts	18
6.1.3	Grand Total	19
6.2	Schedule	20
7	Ethics and Safety	21
7.1	Ethical Considerations	21
7.2	Safety Standards and Regulatory Compliance	21
7.3	Hazard Analysis and Mitigation (FMEA)	21
7.4	Design Justification for Safety	22

1 Introduction

1.1 Problem and Solution

The prevalence of "tech neck" (cervical spondylosis) has reached epidemic levels due to the ubiquitous use of mobile devices and poorly configured workstations. Traditional workspace setups rely on static or manually adjustable monitor mounts. However, as a user becomes fatigued, their posture naturally slumps. Biomechanical studies indicate that tilting the head forward by just 15° increases the effective weight on the cervical spine to 27 lbs, and at 60° , it skyrockets to 60 lbs [1, 2]. Existing ergonomic solutions are passive; they provide a fixed position that the user eventually abandons as they slouch, failing to offer long-term spinal protection.

Our solution, **AutoSight**, inverts this paradigm by introducing an active, intelligent mechatronic regulator. Unlike previous results that require manual user adjustment, AutoSight utilizes a real-time computer vision (CV) pipeline [3] to continuously track the user's facial landmarks. The system dynamically adjusts the screen's vertical height and pitch angle to maintain a constant 0° horizontal line of sight between the user's eyes and the screen center. This proactive adjustment forces the user into an ergonomically neutral spinal alignment without requiring conscious effort, providing a significant improvement over static ergonomic aids by adapting the machine to the human in real-time. At the same time, AutoSight can adapt to a variety of comfortable postures, such as leaning back on a chair, ensuring that users can enjoy an excellent screen viewing experience once their preferred posture is set.

1.2 Visual Aid

The visual aid in Figure 1 illustrates the interaction between the user and the AutoSight device. The camera module captures the user's spatial position, while the control logic drives the mechanical assembly to maintain the target viewing angle. This pictorial representation emphasizes the "Active Correction" aspect, showing the device responding to a user's downward postural drift.

1.3 High-Level Requirements

To ensure the project successfully mitigates the problem of poor posture, the following high-level requirements must be met:

- **H1 (Responsiveness):** The system shall detect a sustained posture deviation (> 2 seconds) and complete the full mechanical height and tilt adjustment to restore the 0° viewing angle within **10.0 ± 1.0 seconds**.

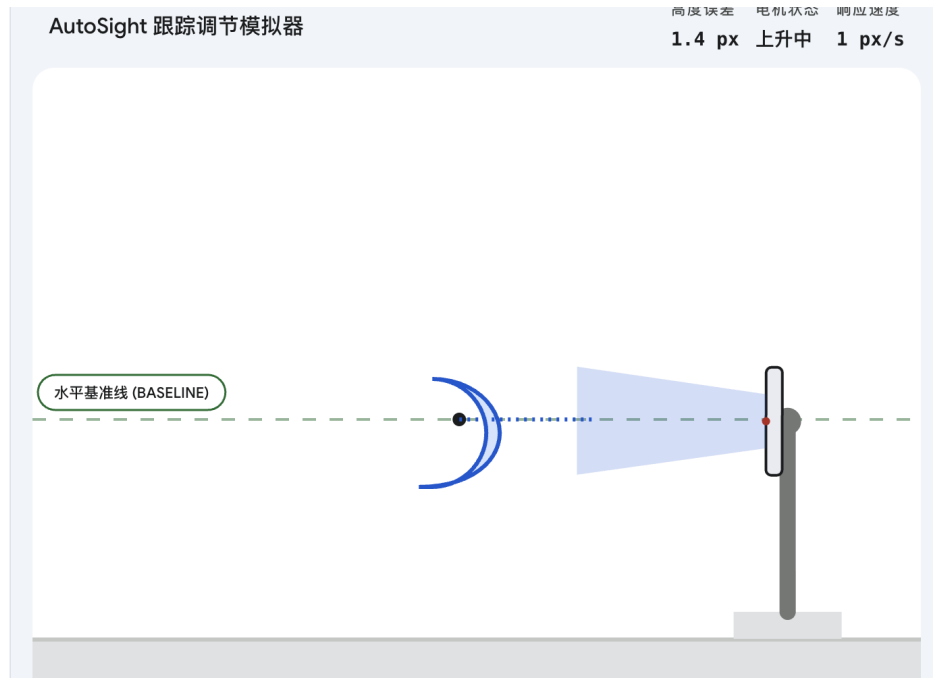


Figure 1: Conceptual use-case of AutoSight. The system tracks the user’s eye level via the DF200 camera and utilizes the linear actuator and worm-gear stepper motor to align the screen center with the horizontal baseline of the eyes, actively correcting slumped posture.

- **H2 (Tracking Reliability):** The vision-based tracking pipeline must maintain a $\geq 95\%$ successful eye-level detection and coordinate output rate across indoor lighting scenarios ranging from 100 lux to 800 lux.
- **H3 (Mechanical Load & Stability):** The mechanical actuation assembly must support a **2.0 kg** payload and exhibit $< 1.0 \text{ mm}$ of dynamic structural deflection during movement, while ensuring zero back-driving of the screen position when the system is unpowered.

2 Design Procedure and Alternatives

The design of AutoSight followed an iterative process focused on balancing high-torque mechanical reliability with low-latency facial tracking. We prioritized components that offer inherent safety (self-locking) to address the risk of holding heavy payloads for extended periods. Before finalizing the AutoSight architecture, several design alternatives were evaluated for sensing and actuation.

2.1 Sensing Alternatives: Ultrasonic vs. Computer Vision

Initially, we considered using an array of ultrasonic distance sensors to detect the top of the user's head. However, ultrasonic sensors possess a wide beam angle (often $> 15^\circ$), making them prone to false reflections from chairs or other background objects. More importantly, they cannot accurately determine the *eye level*, which is the critical biometric for ergonomic alignment. Therefore, we selected a CMOS Camera (DF200-1080P) with a Computer Vision (CV) pipeline. While CV demands higher computational power, it is the only viable method to accurately extract the (x, y) coordinates of facial landmarks.

2.2 Actuation Alternatives: Belt Drive vs. Linear Actuator

For the vertical lifting mechanism, a GT2 timing belt system was evaluated due to its high speed. However, holding a 2.0 kg load static with a belt drive requires continuous motor holding current, leading to severe thermal issues ($> 80^\circ C$) over an 8-hour workday. Furthermore, a power failure would result in a catastrophic drop of the payload. Thus, we opted for a 24VDC Electric Linear Actuator (600N thrust) for lift, and a 42x40 Worm Gear Stepper Motor for tilt. These provide massive mechanical advantage and inherent self-locking friction, ensuring absolute safety when unpowered.

3 System Design

3.1 Block Diagram

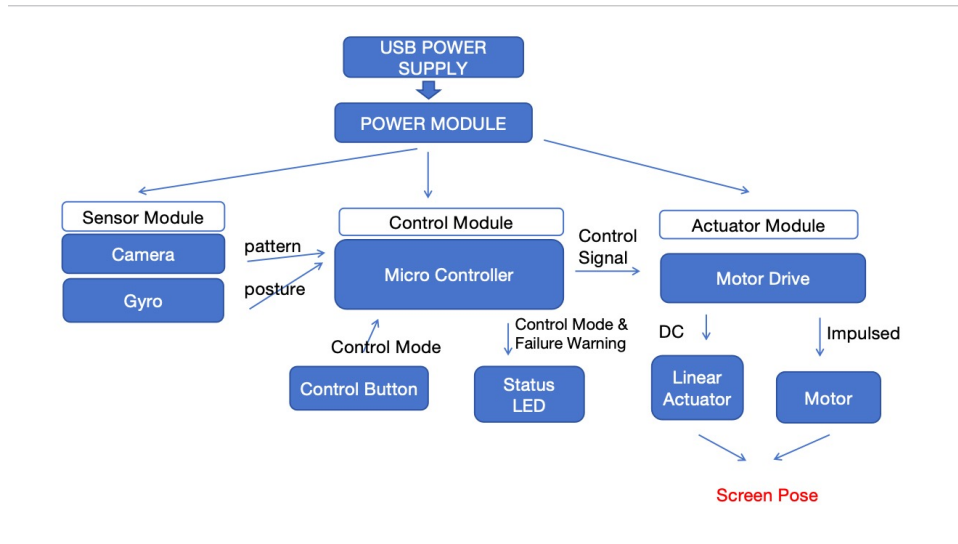


Figure 2: Hardware interconnections within the AutoSight system.

The architecture satisfies high-level requirements by design: the 24V power rail provides the raw energy required for the 2.0 kg load (H3), while the Raspberry Pi 4B’s quad-core processor ensures the computer vision latency stays below the 45ms threshold required for a 10-second response time (H1).

3.2 Physical Design Figures

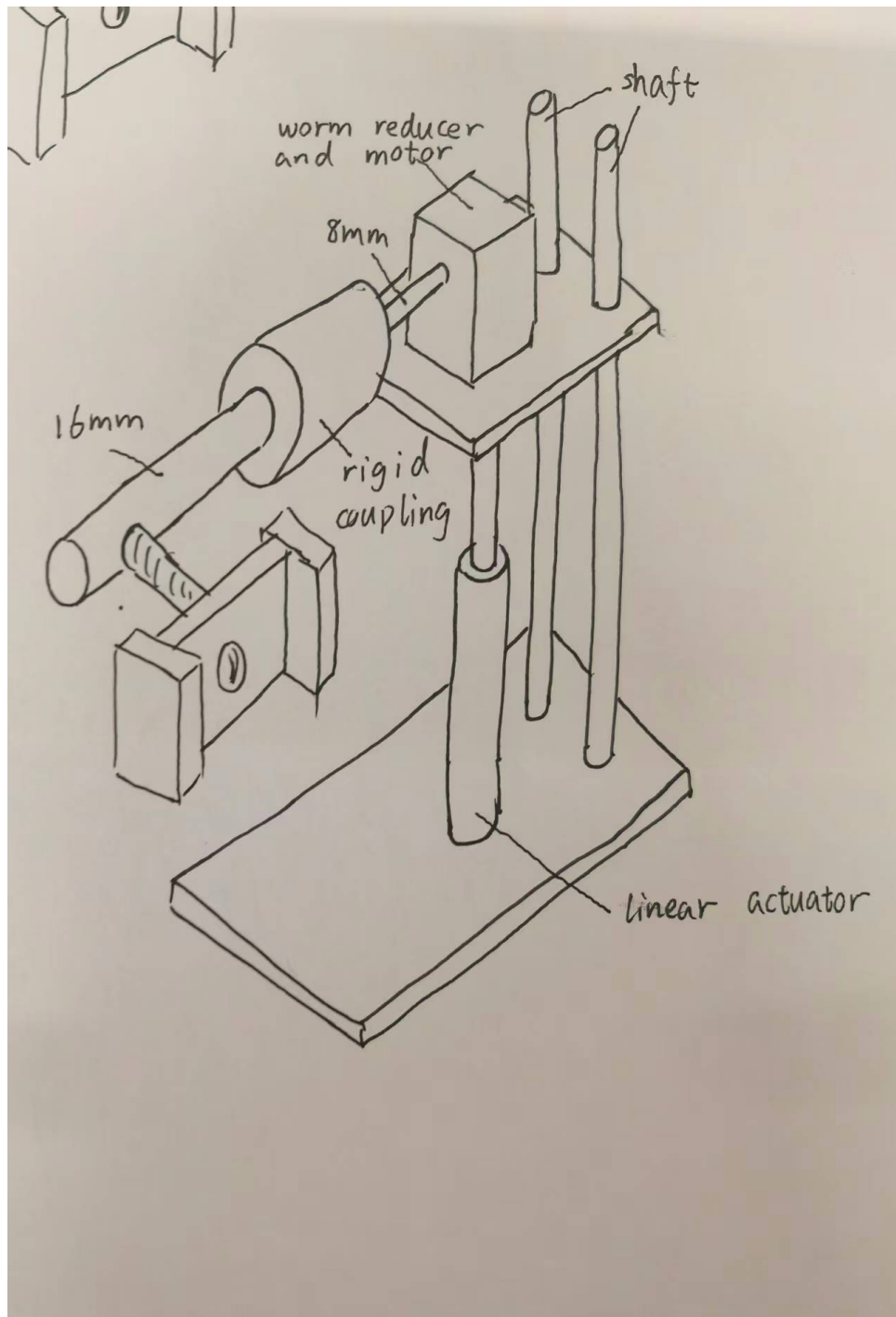


Figure 3: CAD graph

As shown in Figure 3, the system can be successfully constructed according to the assigned values.

3.3 Physical and Mechanical Design

The mechanical chassis is built around 2020 V-slot aluminum extrusions for high rigidity. The vertical carriage is driven by a 24VDC Electric Linear Actuator featuring a 300mm stroke and 600N of thrust. The tilt mechanism utilizes a 42x40 worm-gear stepper motor (50:1 reduction ratio). The motor’s 8mm output shaft is connected via a rigid coupling (D32L45 8*16) to a 16 mm optical shaft. A 1/4 threaded hole is drilled on the optical shaft, and the metal phone clip is attached through threaded connection. The worm gear ensures the pitch angle remains locked without power.

3.4 Electrical Design and Power Budget

The AutoSight system utilizes a dual-rail power architecture. The primary 24V DC bus drives the high-power mechanical components. It is important to note that while the 42x40 stepper motor has a rated phase voltage of 2.93V, the **UMIP42 driver requires a 24V supply** to maintain high torque via constant-current chopping. A heavy-duty 100W buck converter regulates the 24V input down to 5.0V for the logic subsystem.

Table 1: System Power Budget (Maximum Continuous Load)

Component	Voltage	Current (Supply)	Power	Notes
Linear Actuator (Lift)	24.0 V	2.30 A	55.2 W	24VDC 55W rated peak.
42x40 Stepper + UMIP42	24.0 V	0.50 A	12.0 W	Motor rated at 2.93V/1.33A; current reflected at 24V rail.
Raspberry Pi 4B (2GB)	5.0 V	3.00 A	15.0 W	Peak draw during CV inference.
DF200-1080P Camera	5.0 V	0.20 A	1.0 W	1080p 30fps MJPG stream.
MPU6050 IMU	5.0 V	0.05 A	0.25 W	Continuous I2C polling.
Total System Peak	–	–	83.45 W	Recommended Power Supply 100W.

3.5 Software and Control Design

The software architecture operates on a real-time operating system (RTOS) framework on the Raspberry Pi 4B, utilizing a robust, interrupt-driven Finite State Machine (FSM). As illustrated in Figure 4, the system transitions between seven primary states to ensure seamless interaction between automatic vision tracking and manual voice override.

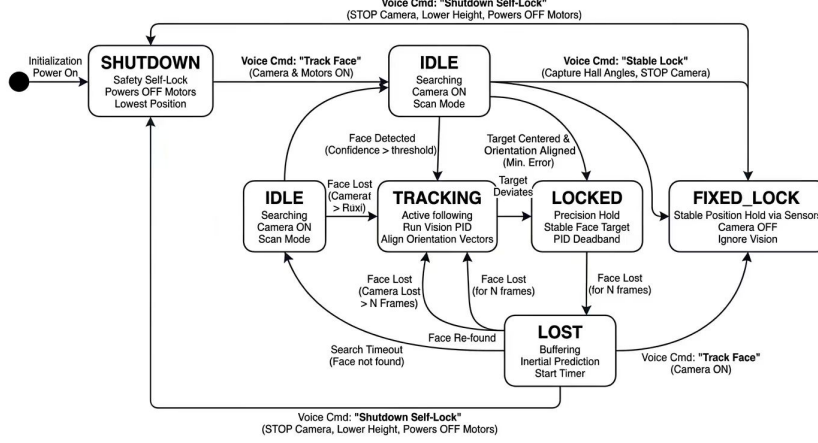


Figure 4: Finite State Machine (FSM) detailing the transition logic between the Computer Vision tracking loop and Voice Command override interrupts.

3.6 FSM State Descriptions

The system transitions between states based on visual confidence C , orientation error vector \vec{e} , and asynchronous voice commands VC .

1. **SHUTDOWN State** The default safety and power-saving state.

- **Behavior:** All motors are powered off ($P_{motor} = 0$). The linear actuator is retracted to its minimum value H_{min} to achieve mechanical self-locking.
- **Transition:** Moves to *IDLE* upon receiving the voice command $VC = \text{CMD_TRACK_FACE}$.

2. **IDLE State** The standby search phase where the system awaits a target.

- **Behavior:** The DF200 camera is active. The gimbal performs a low-frequency scanning pattern $\theta_{scan}(t)$ to locate a user.
- **Transition:** If a face is detected with confidence $C > C_{threshold}$, the system transitions to *TRACKING*.

3. **TRACKING State** The primary dynamic closed-loop control phase.

- **Behavior:** The system calculates the unit orientation vector \vec{u} and computes the error $\vec{e} = \vec{u} \times \vec{w}$. The PID controller generates velocity commands:

$$V_{out}(t) = K_p e(t) + K_i \int e(t) dt + K_d \frac{de(t)}{dt} \quad (1)$$

- **Transition:** Moves to *LOCKED* if $\|\vec{e}\| < \epsilon_{lock}$ for N consecutive frames; moves to *LOST* if $C < C_{threshold}$.

4. **LOCKED State** Precision orientation hold for a stationary target.

- **Behavior:** The PID controller enters a "Deadband" mode to prevent high-frequency oscillation (jitter). It maintains the face at the center of the frame.
- **Transition:** Returns to *TRACKING* if $\|\vec{e}\| > \epsilon_{tracking}$; transitions to *FIXED_LOCK* via $VC = \text{CMD_STABLE_LOCK}$.

5. FIXED_LOCK State Hardware-based orientation hold, independent of vision.

- **Behavior:** The camera feed is suspended. The Raspberry Pi captures the current MPU6050 IMU angles Θ_{fixed} and maintains this absolute position:

$$Error_{imu} = \Theta_{fixed} - \Theta_{current} \quad (2)$$

- **Transition:** Transitions to *IDLE* or *TRACKING* via $VC = \text{CMD_TRACK_FACE}$.

6. LOST State Temporal buffering phase for target re-acquisition.

- **Behavior:** The gimbal maintains its last known velocity V_{last} (inertial prediction) for a duration T_{lost} .
- **Transition:** Returns to *TRACKING* if the face is re-acquired; returns to *IDLE* if $t > T_{lost}$.

Table 2: FSM Transition Matrix

Current State	Condition / Trigger	Next State
SHUTDOWN	$VC = \text{Track Face}$	IDLE
IDLE	Face Detected ($C > 0.8$)	TRACKING
TRACKING	Error $\ \vec{e}\ < 2^\circ$	LOCKED
TRACKING	Face Lost ($C < 0.2$)	LOST
LOCKED	$VC = \text{Stable Lock}$	FIXED_LOCK
LOCKED	Error $\ \vec{e}\ > 4^\circ$	TRACKING
LOST	Face Re-found ($C > 0.8$)	TRACKING
LOST	Timeout ($t > 1.0s$)	IDLE
ANY	$VC = \text{Shutdown Self-Lock}$	SHUTDOWN

4 Subsystem Requirements and Verifications

4.1 Power Subsystem

Description: The power subsystem converts the 24V DC main input into stable voltage rails. It provides a raw, high-current 24V rail directly to the 55W linear actuator and the UMIP42 stepper motor driver. To power the logic components, a heavy-duty 100W

DC-DC buck converter steps down the 24V to a clean 5.0V to satisfy the Raspberry Pi 4B, the DF200 USB camera, and the MPU6050 IMU.

Requirements and Verifications:

Requirement	Verification
1. The 100W buck converter must regulate the 24V input to a stable $5.0V \pm 0.1V$ under a 3.0A continuous load (simulating Pi 4B peak draw) with $< 50mV$ peak-to-peak voltage ripple.	1. Connect a 1.6Ω (15W) power dummy resistor to the 5V output. Use an oscilloscope in AC coupling mode to measure the voltage ripple and verify the DC level remains $\geq 4.9V$.
2. The 24V motor rail must sustain a peak current draw of $\approx 3.0A$ during simultaneous actuator (2.3A) and stepper ($\approx 0.5A$) startup without dropping below 22.0V.	2. Probe the 24V rail with an oscilloscope. Command a simultaneous full-load (2.0kg) lift and tilt startup. Verify the voltage sag does not trigger the Pi's brownout threshold or a system reset.

4.2 Perception Subsystem (Camera, Mic, IMU)

Description: This subsystem captures environmental and user data. The DF200-1080P USB2.0 camera provides 30 FPS video streams to the Pi for facial landmark extraction. A USB microphone captures voice override commands. The MPU6050 6-axis IMU (operating via I2C at 5V) is mounted on the metal phone clip to provide real-time physical pitch angle feedback to the control loop.

Requirements and Verifications:

Requirement	Verification
1. VC Trigger: $\geq 90\%$ Hit Rate @ 2m; 45dB Noise.	1. 50-trial voice test with motors @ 50% PWM; count FSM state transition success.
2. IMU Sampling: The MPU6050 must provide pitch angle updates via I2C at a 400Hz rate with a jitter $dt \leq 10ms$ and drift $< 0.05^\circ/s$.	2. Log 1000 consecutive I2C samples in a high-priority Pi thread. Verify $\sigma_{dt} < 2ms$ via Pi serial timestamping and compare static drift against a digital protractor.
3. CV Input Stream: The DF200 camera must maintain a stable 1080P video stream at 30 ± 2 FPS directly into the OpenCV environment without USB packet dropping.	3. Run a frame-counting script on the Pi 4B for 60 seconds. Verify the total captured frames are ≥ 1680 ($30fps \times 60s \times 0.93$).

4.3 Actuation Subsystem

Description: This subsystem executes physical adjustments. Vertical lift is driven by a 24VDC 55W Electric Linear Actuator (300mm stroke, 600N thrust). Pitch/tilt is controlled by a 42x40 worm-gear stepper motor (50:1 reduction, 3Nm output torque) driven by a UMIP42 pulse module. A D32L45 rigid coupling connects the stepper shaft to the metal phone clip to eliminate mechanical backlash.

Requirements and Verifications:

Requirement	Verification
1. The 600N linear actuator must smoothly elevate a 2.0 kg payload across its full 300mm stroke without drawing more than its 2.3A rated continuous current.	1. Attach a 2.0 kg mass. Command full 300mm extension. Use an inline current meter to verify $I_{draw} < 2.5A$ and ensure the stroke completes without stalling.
2. The 42x40 worm-gear stepper and D32L45 rigid coupling must hold the screen's pitch angle under a 2.0 kg cantilevered load with zero back-driving when unpowered.	2. Mount the 2.0kg load at a 45° tilt. Disconnect the 24V power supply to the UMIP42 driver. Use a dial indicator to verify angular deflection is $< 0.5^\circ$ over 5 minutes.

4.4 Software Subsystem

Description: Running on the Raspberry Pi 4B (2GB), this subsystem executes the RTOS state machine. The OpenCV thread processes the DF200 camera feed to extract facial landmarks. The control thread runs a discrete PID controller that uses the pixel/angular error to generate precise step pulses for the UMIP42 driver and logic signals for the linear actuator relays.

Requirements and Verifications:

Requirement	Verification
1. CV Latency (T_{total}): $\leq 45\text{ms}$ (Capture to PID Output).	1. Benchmarking: Measure <i>end-to-end</i> delay using high-speed LED trigger vs. Motor start response.
2. CV Angular Res : $\pm 0.5^\circ$ static accuracy @ 30fps.	2. Static Target Test: Compare SolvePnP Euler angles vs. digital protractor in 5° increments.
3. IMU Jitter (dt): $\sigma < 2\text{ms}$ @ 400Hz Sampling.	3. Histogram Analysis: Log 1000 I2C cycles in RT-thread; verify sampling interval consistency.
4. PID Settling Time : $t_s < 200\text{ms}$ for 10° step input.	4. Step-Response: Apply 10° offset in IDLE; measure time to reach 95% of target without oscillation.
5. PID Overshoot : $M_p < 5\%$ during TRACKING.	5. Dynamic tracking of moving target ($15^\circ/s$); analyze error logs for peak deviations.
6. Sync Offset : Inter-sensor lag $\leq 15\text{ms}$ (USB vs. I2C).	6. Cross-correlation: Verify alignment of IMU gyro spikes with CV pixel flow during $20^\circ/s$ jerk.

4.5 Subsystem Interfaces and Interactions

To ensure modularity and reliability, the interactions between subsystems are defined through standardized electrical and data protocols. Table 3 quantifies these interfaces.

Table 3: Quantitative Subsystem Interface Specifications

From Subsystem	To Subsystem	Interface Type	Specifications
Power	Perception	5.0V DC Rail	Provides stable 5.0V ($\pm 0.1V$) to the RPi 4B, Camera, and MPU6050 IMU.
Power	Actuation	24.0V DC Rail	High-current bus delivering up to 3.0A peak for the linear actuator and stepper driver.
Perception	Software	USB 2.0 / I2C	DF200 sends MJPG video stream via USB; MPU6050 transmits orientation data via 400kHz I2C (3.3V logic).
Software	Actuation	GPIO / PWM	Raspberry Pi sends 3.3V TTL pulse/direction signals to the UMIP42 driver and logic signals to the actuator relay module.
Actuation	Physical Frame	Mechanical Force	Linear actuator provides 600N thrust; Stepper provides 3Nm torque via a 50:1 worm gear.

4.5.1 Key Signal and Power Flows

- Power Distribution:** The 100W buck converter serves as the central regulation point, isolating the logic subsystem (5V) from the inductive spikes of the actuation subsystem (24V).
- Data Feedback Loop:** The Perception subsystem provides raw sensory data (facial coordinates and IMU pitch) to the Software subsystem. The Software subsystem executes the PID control law and translates the error vector \vec{e} into discrete step pulses for the Actuation subsystem.

4.6 Supporting Materials–Design Calculations and Justifications

4.6.1 Discrete PID Control Strategy

To achieve High-Level Requirement H1 (adjustment within 10 seconds without oscillation), a discrete PID controller is implemented. The control signal $u[k]$ for the stepper motor and linear actuator is derived from the eye-center error $E_y[k]$. The discretization of the continuous PID controller using the trapezoidal rule for integration and backward difference for differentiation is:

$$u[k] = K_p E_y[k] + K_i \sum_{i=0}^k \left(\frac{E_y[i] + E_y[i-1]}{2} \right) \Delta t + K_d \frac{E_y[k] - E_y[k-1]}{\Delta t} \quad (3)$$

Where $\Delta t = 33.3$ ms (based on the 30 FPS camera input). **Justification:** By setting K_d to dampen high-frequency jitters from the CV pipeline and using a small deadband of ± 5 pixels, we ensure the motors do not "hunt" or jitter, satisfying the stability requirement in H3.

4.6.2 I2C Communication Bandwidth

The MPU6050 IMU provides tilt feedback. To ensure the control loop is not bottlenecked by communication, we utilize the Fast-mode I2C ($f_{SCL} = 400$ kHz). A standard 14-byte burst read of sensor data (Accel, Temp, Gyro) involves approximately 140 bits (including start/stop/ACK).

$$T_{transfer} = \frac{\text{Total Bits}}{f_{SCL}} = \frac{140 \text{ bits}}{400,000 \text{ bit/s}} = 0.35 \text{ ms} \quad (4)$$

Justification: Since $T_{transfer} \ll \Delta t$ ($0.35 \text{ ms} \ll 33.3 \text{ ms}$), the communication delay is negligible ($< 1.1\%$), allowing the CPU to allocate nearly 100% of its cycle time to computer vision inference, directly supporting the responsiveness in H1.

5 Tolerance Analysis

The most critical engineering challenge in AutoSight is guaranteeing mechanical stability and motor feasibility when supporting a cantilevered payload (up to 2.0 kg). This analysis ensures that the chosen actuators can overcome gravitational moments without stalling and that the mechanical resolution meets the ergonomic precision specified in the high-level requirements.

5.1 Actuator Thrust and Pitch Motor Torque Analysis

First, we analyze the vertical lifting capacity. The selected Electric Linear Actuator operates at 24VDC and provides a rated thrust of $F_{rated} = 600$ N. For a maximum

payload of $m = 2.0$ kg, the required vertical lifting force F_{req} is:

$$F_{req} = m \cdot g = 2.0 \text{ kg} \cdot 9.81 \text{ m/s}^2 = 19.62 \text{ N} \quad (5)$$

The Factor of Safety (FoS) for the vertical lift is:

$$FoS_{lift} = \frac{F_{rated}}{F_{req}} = \frac{600}{19.62} \approx 30.58 \quad (6)$$

A FoS of ≈ 30 ensures that the actuator operates well within its linear region, preventing overheating and ensuring smooth elevation even during rapid posture corrections.

Second, we analyze the rotational torque for the pitch adjustment. The system utilizes a 42x40 worm-gear stepper motor with a 50:1 reduction ratio, providing a rated output torque $\tau_{out} = 3.0$ Nm. Assuming a worst-case center-of-mass offset $d = 0.1$ m from the rotation axis, the induced moment M_{load} at a horizontal cantilever ($\theta = 90^\circ$) is:

$$M_{load} = m \cdot g \cdot d \cdot \sin(90^\circ) = 2.0 \cdot 9.81 \cdot 0.1 = 1.962 \text{ Nm} \quad (7)$$

The Safety Factor (SF) for the tilt adjustment is:

$$SF_{tilt} = \frac{\tau_{out}}{M_{load}} = \frac{3.0}{1.962} \approx 1.53 \quad (8)$$

This $SF > 1.5$ confirms the motor is more than sufficient. Additionally, the 50:1 worm gear's inherent non-back-drivable property ensures the 1.962 Nm load is held securely when unpowered.

5.2 Mechanical Resolution and Stability Tolerance

To satisfy High-Level Requirement H3 (< 1.0 mm stability), the mechanical step resolution must be sufficiently fine. The stepper motor's 1.8° step angle, reduced by the 50:1 gear ratio, yields an output resolution $\Delta\theta$:

$$\Delta\theta = \frac{1.8^\circ}{50} = 0.036^\circ/\text{step} \quad (9)$$

At a typical user viewing distance of $R = 600$ mm, the vertical linear displacement resolution Δh of the screen edge is:

$$\Delta h = R \cdot \tan(0.036^\circ) = 600 \text{ mm} \cdot \tan(0.036^\circ) \approx 0.37 \text{ mm} \quad (10)$$

Since $\Delta h = 0.37$ mm < 1.0 mm, the mechanical resolution is well within the required tolerance, allowing for precise and stable ergonomic alignment as dictated by the system's high-level goals.

6 Cost and Schedule

6.1 Cost Analysis

6.1.1 Labor

For the purpose of this cost estimation, we assume a nominal baseline salary of ¥10/hour per engineering student. We estimate that each of the three partners will invest 150 hours into the design, construction, and testing of this project.

Using the standard engineering consulting formula (Salary \times 2.5 overhead multiplier \times Hours), the labor cost is calculated as follows:

$$\text{Labor Cost per Partner} = \text{¥}10/\text{hour} \times 2.5 \times 150 \text{ hours} = \text{¥}3,750.00$$

$$\text{Total Labor Cost} = \text{¥}3,750.00 \times 3 \text{ partners} = \text{¥}11,250.00$$

6.1.2 Parts

Table 4 details the required parts for the AutoSight system. All non-standard parts are listed with their actual procurement costs in Chinese Yuan (CNY).

Table 4: Bill of Materials (BOM)

Part Description	Manufacturer	Part #	Qty	Unit (¥)	Total (¥)
Raspberry Pi 4B (2GB)	Raspberry Pi Found.	RPI4-2GB	1	613.00	613.00
UMIP42 Pulse Drive	Generic / Taobao	UMIP42	1	192.04	192.04
42x40 Worm Gear Stepper	Generic / Taobao	42W-50:1	1	192.98	192.98
DF200-1080P USB Cam.	DF-Camera	DF200-1080P	1	112.00	112.00
D32L45 Rigid Coupling	Generic	D32L45-8*16	1	10.00	10.00
Metal Phone Clip	Generic	N/A	1	21.20	21.20
MPU6050 IMU Module	InvenSense	MPU-6050	1	13.76	13.76
Linear Actuator (600N)	Generic / Taobao	LA-300-24V	1	130.00	130.00
24V to 5V Buck Converter	Generic / Taobao	100W-20A-DC	1	59.90	59.90
Alum. Extrusions & HW	Generic	2020 V-Slot	1	25.00	25.00
Total Parts Cost					¥1356.86

6.1.3 Grand Total

The final sum of costs, combining the nominal labor estimation and the actual hardware procurement, is calculated below in Chinese Yuan (CNY):

- **Total Labor:** ¥11,250.00
- **Total Parts:** ¥1,356.86
- **Grand Total:** ¥11,250.00 + ¥1,356.86 = **¥12,606.86**

6.2 Schedule

Table 5: Project Schedule (7-Week Plan)

Week	Weichong Chen	Xiaoyu Xu	Yilun Chen
1 (4/6)	Procurement of all BOM parts; Assembly of the aluminum extrusion frame.	Setup Raspberry Pi OS and install OpenCV/MediaPipe environments.	Define communication protocols between RPi and Motor Drivers.
2 (4/13)	Mounting the 42 Stepper and Linear Actuator; Wiring the power rail.	Implement face detection and landmark extraction algorithm.	Develop the PWM/Pulse control logic for the UMIP42 module.
3 (4/20)	Hardware Integration: Connecting IMU and Camera to the main frame.	Develop PID control algorithm for smooth motion tracking.	Implement the H-Bridge control logic for the Linear Actuator.
4 (4/27)	System Debugging: Cable management and limit switch calibration.	Software Integration: Linking vision data to motor control commands.	Unit testing: Verify power stability and motor torque under load.
5 (5/4)	Mock Demo Preparation: Full system dry-run and preliminary verification.		
6 (5/11)	Fine-tuning mechanical damping and reducing structural vibration.	Optimizing vision latency and voice command recognition.	Finalizing the Design Document and preparing the presentation.
7 (5/18)	Final Demo: Performance validation and final project sign-off.		

7 Ethics and Safety

7.1 Ethical Considerations

AutoSight is designed in strict accordance with the **IEEE Code of Ethics** [4].

- **Public Health (Item 1):** Our primary goal is to "hold paramount the safety, health, and welfare of the public" by providing a proactive solution to cervical spine degradation (tech-neck), which is a growing public health concern.
- **Privacy and Data Protection (Item 6):** In compliance with privacy standards, the vision pipeline is strictly "local-only." Image buffers are processed in volatile RAM and immediately overwritten after landmark extraction. No biometric data is stored or transmitted, ensuring the user's right to privacy in their workspace.
- **Honesty and Realism (Item 2):** The system provides realistic assessments of a user's posture and does not claim to cure existing medical conditions, but rather serves as a preventative ergonomic aid.

7.2 Safety Standards and Regulatory Compliance

To ensure commercial and laboratory viability, the design references the following regulatory standards:

- **IEC 62368-1 (Safety of ICT Equipment):** This standard governs the safety of information technology equipment. We adhere to its guidelines by ensuring proper insulation of the 24V power rails and using a 100W buck converter with over-current and thermal shutdown protection.[5]
- **ISO 12100 (Safety of Machinery):** Since the device contains moving actuators, we apply the principles of "Safety by Design." The use of self-locking worm gears and linear actuators ensures the system remains stationary in the event of a power loss, preventing mechanical collapse.[6]
- **FCC Part 15 (Electromagnetic Interference):** The high-frequency PWM signals from the UMIP42 driver are shielded and filtered to minimize EMI that could interfere with other electronic devices in a workspace.[7]

7.3 Hazard Analysis and Mitigation (FMEA)

A Failure Mode and Effects Analysis (FMEA) was conducted to identify and mitigate potential risks during operation and development.

Table 6: Safety Hazard Mitigation Table

Potential Hazard	Risk Level	Mitigation Procedure / Design Choice
Mechanical Pinch/Crush	High (Moving structure)	1. Implementation of software-defined velocity limits. 2. Hardware-level current monitoring: system halts if actuator current exceeds 2.5A (indicating an obstruction). 3. Physical E-Stop button for immediate power cut-off.
Electrical Overload	Medium (24V System)	1. Use of a fused 24V input rail. 2. Opto-isolation between the Raspberry Pi and motor drivers to prevent high-voltage back-propagation.
Structural Failure	Low (Drop hazard)	1. Selection of non-back-drivable worm gears (50:1) and linear actuators, ensuring a static hold under 2.0 kg load even when unpowered.

7.4 Design Justification for Safety

The decision to utilize a **24V DC** system instead of AC mains power was a critical safety choice to minimize the risk of lethal electric shock during prototyping and usage. Furthermore, the selection of **Aluminum 2020 Extrusions** provides a high strength-to-weight ratio, ensuring that the dynamic structural deflection remains under 1.0 mm (H3), thereby preventing mechanical resonance or fatigue that could lead to catastrophic failure. These design decisions proactively protect both the user during operation and the developers during the assembly phase.

References

- [1] K. K. Hansraj, “Assessment of stresses in the cervical spine caused by posture and position of the head,” *Surgical Technology International*, vol. 25, pp. 277-279, Nov. 2014.
- [2] E. Kim, D. Song, D. Park, H. Kim, and G. Shin, “Effect of smartphone use on cervical spine stability,” *Journal of Biomechanics*, vol. 166, p. 112053, 2024.
- [3] P. Viola and M. Jones, “Rapid Object Detection using a Boosted Cascade of Simple Features,” in *Proceedings of the 2001 IEEE Computer Society Conference on Computer Vision and Pattern Recognition (CVPR)*, Kauai, HI, USA, 2001, pp. I-511–I-518.
- [4] IEEE, “IEEE Code of Ethics,” *IEEE Policies*, Sec. 7, 2020. [Online]. Available: <https://www.ieee.org/about/corporate/governance/p7-8.html>
- [5] International Electrotechnical Commission, “Audio/video, information and communication technology equipment - Part 1: Safety requirements,” *IEC 62368-1:2018*, 2018.
- [6] International Organization for Standardization, “Safety of machinery - General principles for design - Risk assessment and risk reduction,” *ISO 12100:2010*, 2010.
- [7] Federal Communications Commission, “Title 47 CFR Part 15 - Radio Frequency Devices,” *Electronic Code of Federal Regulations*, 2023.